Reprinted from Chemistry of MATERIALS, 1995, 7.

Photophysical Properties, Self-Assembled Thin Films, and Light-Emitting Diodes of Poly(*p*-pyridylvinylene)s and Poly(*p*-pyridinium vinylene)s

Jing Tian,[†,⊥] Chung-Chih Wu,[‡] Mark E. Thompson,*[,†] James C. Sturm,[‡] and Richard A. Register[§]

Advanced Technology Center for Photonic and Optoelectronic Materials (POEM), Princeton University, Princeton, New Jersey 08544

Received June 26, 1995. Revised Manuscript Received September 5, 1995[⊗]

Poly(*p*-pyridylvinylene) (PPyV) and its derivatives have been synthesized, and their optical properties have been studied in solutions and thin films. These conjugated polymers are highly photoluminescent in both their neutral and protonated states. Polymer thin films and concentrated solutions show photoluminescence (PL) from excimeric states, which contributes to the observed red-shift in the emission spectra and the low PL quantum yields relative to dilute solutions. Self-assembled polymer thin films of poly(pyridinium vinylene) with sulfonated polystyrene or sulfonated polyaniline have been prepared by the electrostatic deposition method. Various deposition conditions were investigated and the films examined by atomic force microscopy (AFM). Light-emitting devices (LEDs) with several different architectures were made from this class of polymers and evaluated. The polymer thin films were spin-coated from solution, and the devices emit generally orange-red colors consistent with their PL spectra. The device made from poly(3-n-butyl-*p*-pyridylvinylene) with the configuration ITO/Bu-PPyV/Al has an external quantum efficiency of 0.02%. The introduction of a hole transport layer (poly(*p*-phenylenevinylene), PPV) between the Bu–PPyV and ITO layers improves the quantum efficiency of the device (up to 0.05%), reduces the operating voltage and prolongs the life of the device.

Introduction

There has been a great deal of interest in using organic materials in light-emitting diodes (LEDs) because of their low cost, ease of fabrication, low operating voltages, and good quantum efficiencies. Both organic molecular materials and polymers have demonstrated promise as emitting materials in LEDs. Poly(*p*-phenylenevinylene) (PPV) was the first conjugated polymer reported to serve as an emissive layer in an LED.[1] Since that report, a number of different polymers have been synthesized and extended efforts have been made to obtain high performance devices from polymeric materials.[1–17]

There are a number of different factors influencing the performance of LEDs. Factors such as the fluorescence quantum efficiency, charge carrier mobility, and thermal stability are inherent to the emitting materials. Other factors are intrinsic to the device design and the method of preparation. The configuration of the devices, the thickness and the uniformity of the emitting and injection layers, the composition of the contact electrodes[9] and the carrier injection layers[18,19] are examples of such factors. A number of different factors affect the efficiency and color of organic LEDs, which can be controlled by alteration of the organic materials. Such chemical tuning of properties can be seen in cyano-

† Department of Chemistry.
‡ Department of Electrical Engineering.
§ Department of Chemical Engineering.
⊥ Current address: Raychem Corporation, 300 Constitution Dr., Menlo Park, CA 94025.
* To whom correspondence should be addressed. Permanent address: Department of Chemistry, University of Southern California, Los Angeles, CA 90089.
⊗ Abstract published in *Advance ACS Abstracts,* October 15, 1995.

(1) Burroughes, J. H.; Bradley, D. D. C.; Brown, A. R.; Marks, R. N.; Mackay, K.; Friend, R. H.; Burn, P. L.; Holmes, A. B. *Nature* **1990**, *347*, 539.
(2) Gustafsson, G.; Cao, Y.; Treacy, G. M.; Kavvetter, F.; Colaneri, N.; Heeger, A. J. *Nature* **1992**, *357*, 477.
(3) Yu, G.; Zhang, C.; Heeger, A. J. *Appl. Phys. Lett* **1994**, *64*, 1540.
(4) Burn, P. L.; Holmes, A. B.; Kraft, A.; Bradley, D. D. C.; Brown, A. R.; Friend, R. H.; Gymer, R. W. *Nature* **1992**, *356*, 47.
(5) Vestweber, H.; Greiner, A.; Lemmer, U.; Mahrt, R. F.; Richert, R.; Heitz, W.; Bässler, H. *Adv. Mater.* **1992**, *4*, 661.
(6) Gill, R. E.; Malliaras, G. G.; Wildeman, J.; Hadziioannou *Adv. Mater.* **1994**, *6*, 132.
(7) Grem, G.; Leditzky, G.; Ullrich, B.; Leising, G. *Adv. Mater.* **1992**, *4*, 36.
(8) Yamamoto, T.; Maruyama, T.; Zhou, Z. H.; Ito, T.; Fukuda, T.; Yoneda, Y.; Begum, F.; Ikeda, T.; Sasaki, S.; Takezoe, H.; Fukuda, A.; Kubota, K. *J. Am. Chem. Soc.* **1994**, *116*.
(9) Parker, I. D. *J. Appl. Phys.* **1994**, *75*, 1656.
(10) Bradley, D. D. C. *Adv. Mater.* **1992**, *4*, 756–758.
(11) Hsieh, B. R.; Antoniadis, H.; Bland, D. C.; Feld, W. A. *Adv. Mater.* **1995**, *7*, 36–38.
(12) Hesemann, P.; Vestweber, H.; Pommerehne, J.; Mahrt, R. F.; Greiner, A. *Adv. Mater.* **1995**, *7*, 388–390.
(13) Malliaras, G. G.; Herrema, J. K.; Wildeman, J.; Wieringa, R. H.; Gill, R. E.; Lampoura, S. S.; Hadziioannou, G. *Adv. Mater.* **1993**, *5*, 721–723.
(14) Gill, R. E.; Malliaras, G. G.; Wildeman, J.; Hadziioannou, G. *Adv. Mater.* **1994**, *6*, 132–135.
(15) Berggen, M.; Gustafsson, G.; Inganäs, O.; Anderson, M. R.; Wennerström, O.; Hjertberg, T. *Adv. Mater.* **1994**, *6*, 488–490.
(16) Yang, Z.; Sokolik, I.; Karasz, F. E. *Macromolecules* **1993**, *26*, 1188–1190.
(17) Seggern, H. von; Schmidt-Winkel, P.; Zhang, C.; Parbaz, K.; Kraabel, B.; Heeger, A. J.; Schmidt, H. W. *A. C. S. Polym. Prepr.* **1993**, *34*, 532–533.
(18) Adachi, C.; Tsutsui, T.; Shogo, S. *Appl. Phys. Lett.* **1990**, *56*, 799.
(19) Brown, A. R.; Bradley, D. D. C.; Burroughes, J. H.; Friend, R. H.; Greenham, N. C.; Burn, P. L.; Kraft, A. *Appl. Phys. Lett.* **1992**, *61*.

0897-4756/95/2807-2190$09.00/0

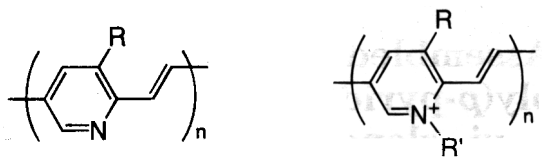

(a) (b)

PPyV: R = H
Me-PPyV: R= CH_3
Bu-PPyV: R = n-C_4H_9

PHPyV: R, R' = H
Bu-PHPyV: R = n-C_4H_9, R' = H
PMePyV: R = H, R' = CH_3

Figure 1. Poly(p-pyridylvinylene)s (a) and oply(p-pyridinium vinylidene)s used in this study. These drawing depict a polymer composed of 100% head-to-tail connections along the polymer backbone (i.e., C2 of one pyridyl group always bridges to C5 of an adjacent pyridyl group). The polymer studied here has all of the pyridyl groups substituted in the 2 and 5 positions to make the chain, but the relationship of adjacent pyridyl groups is random (i.e., C2 of one pyridyl group can be bound to either C5 or C2 of an adjacent group).

substituted poly(arylene vinylenes), which have increased electron affinity, leading to improved electron injection rate and device efficiency.[20] Two challenging problems in developing polymer LEDs are achieving a high luminescent quantum yield and developing methods for fabricating very thin polymer films in a controllable fashion.

Decher and co-workers[21-24] have reported the assembly of multilayer polymer thin films by electrostatic deposition techniques. Self-assembled polymer thin films are fabricated by sequential adsorption of polyanions and polycations onto a charged surface. This technique utilizes electrostatic interactions between charged polymers to assemble a highly uniform film and has been extended to conjugated polymers as well.[25,26] It is possible to build heterostructure thin films with complex molecular architecture and controllable thickness at the molecular level. Recently, Rubner and coworkers have fabricated polymeric light-emitting devices from a self-assembled PPV thin film.[27] In this fabrication a thin film of the PPV precursor was deposited and thermally annealed to give the conjugated polymer.

Herein we report the fluorescent and electroluminescent properties of poly(*p*-pyridylvinylene)s and poly(pyridinium vinylene)s (Figure 1). The charged poly(pyridinium vinylene)s provide the possibility to fabricate polymer thin films by the electrostatic deposition method, without the need for postdeposition thermal treatment. The preparation and characterization of these self-assembled thin films will be discussed. The performance of single layer polymer LEDs made from spin-coated polymer thin films, films prepared by electrostatic deposition as well as heterostructured devices, are evaluated.

Experimental Section

Materials. 3-*n*-Butylpyridine (98%), triphenylphosphine (99%), palladium chloride (99%), *trans,trans*-dibenzylideneacetone (99%), 1-methyl-2-pyrrolidone (NMP) (99+%), sodium amide (90%), *m*-cresol (99%), methanesulfonic acid (MSA) (99%) and trifluoroacetic acid (99%), poly(sodium styrene sulfonate) (PSSNa), and poly(acrylic acid) were obtained from Aldrich Chemicals and used without purification. Poly(methacrylic acid) and poly(ethyleneimine) (PEI) were purchased from Polysciences. Anhydrous cymene was refluxed over CaH_2 and stored under argon prior to use. 2,5-dibromopyridine was purified by recrystallizing from heptane. *E*-1,2-Bis(tributylstannyl)ethylene[28] and palladium(0) bis(dibenzylideneacetone) ($Pd(dba)_2$)[29] were prepared according to the literature procedures. Sulfonated polyaniline (SPANI) was also obtained as described in the literature.[30] Poly(*p*-phenylenevinylene) was synthesized via the precursor route and was annealed in reforming gas (5% hydrogen in nitrogen).[31,32]

Instrumentation. Electronic absorption spectra of polymer solutions and films were measured on an AVIV Model 14DS spectrophotometer (modified Cary-14) The photoluminescence spectra were taken with a Perkin-Elmer Model LS 50 luminescence spectrometer. The front face measurements of PL spectra and time-resolved PL spectra were carried out on a PTI (Photon Technology International Inc.) QM-1 fluorimeter and a SE-910Q Strobemaster fluorescence lifetime system, respectively. The measurements made with PTI equipment were carried out by Dr. Alex Siemiarczuk (Photon Technology International, London, Ontario, Canada). The excitation wavelength used was the maximum absorption wavelength in each electronic absorption spectrum. Proton NMR spectra were obtained on a GE QE-300 spectrometer. AFM images of polymer thin films were obtained on a Digital Instruments Nanoscope III in tapping mode.

Synthesis of Monomers. *2-Amino-3-alkylpyridine*: Both the methyl and *n*-butyl derivatives of this compound were prepared. The synthesis described below is for the butyl derivative but will work equally well if 0.1 mol of 3-methylpyridine is substituted for 3-*n*-butylpyridine. Sodium amide (4.5 g, 0.115 mol) was stirred in 25 mL of anhydrous cymene under argon at 60 °C for 2 h. 3-*n*-Butylpyridine (13.5 g, 0.10 mol) was added to the sodium amide suspension via syringe followed by an addition of cymene (10 mL). The reaction mixture was heated at 170 °C for 20 h to give a thick, dark brown slurry. The mixture was cooled to room temperature and carefully poured onto ice. The mixture was treated with 6 M HCl and the aqueous layer was separated. The organic layer was extracted with 6M HCl (2 × 50 mL), and the combined aqueous solution was made basic with sodium hydroxide solution. This solution was extracted with CH_2Cl_2, dried, and concentrated. The desired product was obtained by vacuum distillation as a colorless liquid which became a pale-yellow solid at room temperature.[33] The NMR spectrum indicates the presence of 6-amino-3-n-butylpyridine (~25%). The mixture was typically used in the synthesis of 2-amino-5-bromo-3-*n*-butylpyridine without further purification. The 6-amino contaminant leads ultimately to a 5,6-dibromopyridine compound. This is removed by recrystallization after the next step. *Purified 2-amino-3-butylpyridine*: yield- 30%. ^1H NMR spectrum, DMSO-d_6 δ 7.86 (doublet, 1H), 7.28 (doublet, 1H), 6.56 (multiplet, 1H), 5.74 (s, 2H), 2.49 (multiplet, 2H), 1.59 (multiplet, 2H), 1.44 (multiplet, 2H), 1.00 (triplet, 3H). Mass spectrum: *m/e*, rel int 150 (M^+), 16.7; 135, 4.6; 121, 7.7; 107, 43.5; 79.99, 44.4.

(20) Greenham, N. C.; Moratti, S. C.; Bradley, D. D. C.; Friend, R. H.; Holmes, A. B. *Nature* **1993**, *365*, 628.
(21) Decher, G.; Hong, J. D.; Schmitt, J. *Thin Solid Films* **1992**, *210/211*, 831.
(22) Lvov, Y.; Decher, G.; Sukhorukov, G. *Macromolecules* **1993**, *26*, 5396.
(23) Lvov, G. Y.; Decher; Möhwald, H. *Langmuir* **1993**, *9*, 481.
(24) Lvov, Y.; Essler, F.; Decher, G. *J. Phys. Chem.* **1993**, *97*, 13773.
(25) Cheung, J. H.; Fou, A. F.; Rubner, M. F. *Thin Solid Films* **1994**, 985.
(26) Ferreira, M.; Cheung, J. H.; Rubner, M. F. *Thin Solid Films* **1994**, *244*, 806.
(27) Fou, A. C.; Onitsuka, O.; Rubner, M. F. *Proc. ANTEC* **1995**, 1594-1595.
(28) Neumann, W. P. *The Organic Chemistry of Tin*; Wiley-Interscience: New York, 1970.
(29) Ukai, T.; Kawazura, H.; Ishii, Y.; Bonnet, J. J.; Ibers, J. A. *J. Organomet. Chem.* **1974**, *65*, 253.
(30) Yue, J.; Epstein, A. J. *J. Am. Chem. Soc.* **1990**, *112*, 2800.
(31) Gagnon, D. R.; Capistran, J. D.; Karasz, F. E.; Lenz, R. W.; Antoun, S. *Polymer* **1987**, *28*, 567.
(32) Papadimitrakopoulos, F.; Konstadinidis, K.; Miller, T. M.; Opila, R.; Chandross, E. A.; Galvin, M. E. *Chem. Mater.* **1994**, *6*, 1563.
(33) Hardegger, E.; Nikles, E. *Helv. Chim. Acta* **1956**, *59*, 505.

2-Amino-5-bromo-3-alkylpyridine. Both the methyl and *n*-butyl derivatives of this compound were prepared. The synthesis described below is for the butyl derivative but will work equally well for the methyl derivative. The above mixture (4.8 g, 0.032 mol) was dissolved in 20 mL of ethanol, and the solution was cooled to 0 °C. To this solution, 1.7 mL (0.032 mol) of Br_2 was added slowly, keeping the reaction temperature below 5 °C. The reaction mixture was held at 0 °C for 1 h after the addition was complete. After removal of the solvent, an orange-yellow gluelike solid was obtained which was washed with dilute NaOH to give a yellow solid.[34] The solid was purified by dissolving in dilute aqueous HCl solution (pH of 4), filtering out any precipitate and adjusting the solution to pH = 9 with NaOH. The precipitate was collected and recrystallized from heptane to give 2-amino-5-bromo-3-*n*-butylpyridine. A second recrystallization removes the remaining traces of 6-amino-5-bromo-3-*n*-butylpyridine (vide supra) from the desired product. *2-amino-3-butyl-5-bromopyridine*: yield 51%. ^{1}H NMR spectrum, DMSO-d_6 δ, 7.87 (3, 1H), 7.38 (doublet, 1H), 6.00 (s, 2H), 2.42 (triplet, 2H), 1.52 (multiplet, 2H), 1.47 (multiplet, 2H), 0.94 (triplet, 3H). Mass spectrum: *m/e*, rel int 230 (M^+), 12.1; 229, 74.7; 228, 16.3; 227, 76.6; 214, 24.5; 212, 28.0; 200,33.4; 198, 35.6; 186, 93.5; 185, 80.2; 184, 93.5, 106, 100.

2,5-Dibromo-3-n-butylpyridine. Both the methyl and *n*-butyl derivatives of this compound were prepared. The synthesis described below is for the butyl derivative, but will work equally well for the methyl derivative. 2-Amino-5-bromo-3-*n*-butylpyridine (5 g, 0.022 mol) was dissolved in 15.4 mL (0.066 mol) of 47% HBr and cooled with an ice bath, forming a white slurry. Br_2 (3.75 mL, 0.066 mol) was added slowly to the solution, the temperature was maintained below 5 °C. The solution changed to a red color and a precipitate was formed. At the end of the addition the precipitate dissolves. Sodium nitrate ($NaNO_2$, 4.62 g, 0.066 mol) of sodium nitrate ($NaNO_2$) was prepared as a saturated aqueous solution which was added to the reaction mixture below 5 °C over a period of ~3 h. Then 9.9 g (0.25 mol) of NaOH in 25 mL of water was added slowly, while keeping the reaction mixture below 20 °C. About 30 mL of ether was used to extract the organic and a brown oily product was obtained upon removal of ether. The colorless liquid product was obtained via vacuum distillation.[34] *2,5-Dibromo-3-butylpyridine*: yield 49%. ^{1}H NMR spectrum, $CDCl_3$ δ, 8.26 (doublet, 1H), 7.61 (doublet, 1H), 2.67 (multiplet, 2H), 1.59 (multiplet, 2H), 1.43 (multiplet, 2H), 0.98 (triplet, 3H). Mass spectrum: 294 (M^+), 80.6; 293, 22.3; 292, 94.5, 290, 82.8; 252, 63.5; 251, 46.3; 250, 90.7; 249, 65.0; 248, 66.5; 247, 37.7; 215, 80.5; 214, 38.9; 213, 85.6, 169, 100.

Synthesis of Polymers. The polymer was synthesized through dehalogenation polycondensation via the cross-coupling reaction between the corresponding 2,5-dibromopyridine and (*E*)-1,2-bis(tributylstannyl)ethylene in the presence of palladium phosphine complex.[35,36] Anhydrous NMP solution (25 mL) containing triphenylphosphine (PPh_3, 0.8 mmol), Pd(dba)$_2$ (0.2 mmol), and 2,5-dibromopyridine (10 mmol) was purged with argon at room temperature and heated to 110 °C. To this solution (*E*)-1,2-bis(tributylstannyl)ethylene (10 mmol) was added and the reaction was refluxed for another 20 h. The polymers (except Bu–PPyV) precipitate during the synthesis. The reaction mixture for Bu–PPyV was taken to dryness by rotary evaporation. The polymer precipitates were purified by soxhlet extraction with hexane, to remove low molecular weight materials. Both PPyV and Me–PPyV are soluble in *m*-cresol and strong acids, such as sulfuric acid, formic acid, and trifluoroacetic acid. For Bu–PPyV, the polymer was first extracted with hexane followed by toluene. Most of the Bu–PPyV polymer was soluble in toluene and a powder was obtained upon removing the toluene solvent.

Polymer Molecular Weights. Gel permeation chromatography measurements employed a Waters M45 pump and Model 481 ultraviolet absorbance detector, which was tuned to the λ_{max} value. The mobile phase was THF flowing at 1.0 mL/min. Two 30 cm polystyrene gel columns (10^3 and 500 Å pore sizes) were used to achieve good separation in the molecular weight range of interest. The columns were calibrated with a series of narrow-distribution polystyrene standards; the molecular weights reported are polystyrene-equivalent values, uncorrected for hydrodynamic volume. The molecular weight found for Bu–PPyV was 5200 g/mol (M_w/M_n = 1.9) and for PPyV was 3000 g/mol (M_w/M_n = 2.2).

Fluorescence Spectra Measurement. Solution fluorescence spectra were mostly measured with right angle excitation. For polymer films the PL spectra were measured by exciting at 90° to the film surface, and the emitted light was collected from the side of the thin film. The solution quantum yield was measured by comparing the integrated emission spectra to that of rhodamine B in ethanol with identical optical density.[37] Photoluminescence quantum yields of Bu–PPyV and Bu–PHPyV were measured with 10^{-6} M THF solutions (based on the monomer repeat unit). The Bu–PHPyV solution was made by adding the stoichiometric amount of MSA to the Bu–PPyV solution. The excitation wavelength used in measuring the PL for polymer solutions was 420 nm and the excitation wavelength used in obtaining the photoluminescence spectrum of rhodamine B was 530 nm.

Fabrication and Testing of LEDs. The Bu–PPyV films were spin-coated onto the ITO-coated glass substrates chloroform or THF solutions (devices made from both solutions gave similar results). Typically, concentrations of 0.1–0.2 M (according to the repeating unit of the polymer) and a spinning rate of 2000–4000 rpm give uniform dark yellow films of 500–1500 Å. The LEDs were finished by vacuum depositing an aluminum electrode on top of the organic film. The base pressure of the chamber was 10^{-6} mbar and the evaporating pressure was 10^{-5} mbar. The thickness of the electrode was ca. 1000 Å and the area of the electrode was 1 mm^2. The *I–V* characteristics of the devices were measured on an HP analyzer (Model HP 4145B) and the EL spectra were collected using an EG&G monochromator and Electrim 1000 TE CCD camera.

The EL efficiency was measured using a 1 cm diameter silicon photodetector, placed 1 mm away from the glass substrate. The measured current was corrected for detector efficiency (0.75 in the green to red part of the spectrum). No further corrections were made for absorption, waveguiding in the glass substrate or other effects that act to decrease the light emitted out of the backside of the glass substrate. Thus all of the quantum efficiencies reported here are external quantum efficiencies. It has been estimated that the total or "internal" quantum efficiencies for devices of this type are 4–5 times greater than the measured external efficiencies.[38]

Results and Discussion

Two of the pyridylvinylene polymers discussed herein have been reported previously (i.e., PPyV and PMePyV).[35] PPyV is quite stable but is only soluble in strong acid solutions and *m*-cresol. While PMePyV is significantly more soluble,[39] it is unstable in the presence of nucleophilic reagents, such as water, dimethylformamide, dimethyl sulfoxide, and dimethylacetamide. To increase the solubility of PPyV, we added an alkyl group to the pyridyl ring. Poly(3-*n*-methyl-*p*-pyridylvinylene) (Me–PPyV) was prepared but showed very little change in solubility relative to PPyV. Substitution of a butyl group for the methyl group leads to a dramatic increase in solubility. Poly(3-*n*-butyl-*p*-pyridylvinylene)

(34) Craig, L. C. *J. Am. Chem. Soc.* **1934**, *56*, 231.
(35) Marsella, M. J.; Fu, D. K.; Swager, T. M. *Adv. Mater.* **1995**, *7*, 145.
(36) Tian, J.; Wu, C.-C.; Thompson, M. E.; Sturm, J. C.; Register, R. A. *Adv. Mater.* **1995**, *7*, 395–398.
(37) Guillbault, G. G. *Practical Fluorescence*; Decker: New York, 1992.
(38) Greenham, N. C.; Friend, R. H.; Bradley, D. D. C. *Adv. Mater.* **1994**, *6*, 491–494.
(39) PMePyV has a $CF_3SO_3^-$ counterion. This polymer is prepared by treating PPyV with $CF_3SO_3CH_3$ as described in ref 35.

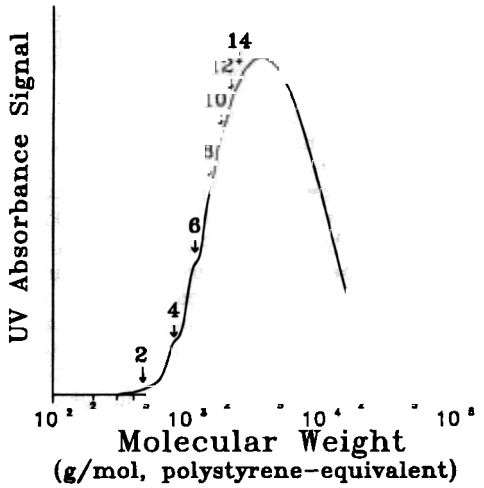

Figure 2. Molecular weight distribution of the Bu-PPyV. Numbers on the horizontal axis correspond to the molecular weights of polystyrene standards having the same elution times. Arrows indicate the presence of discrete oligomers. The spacing between the arrows is 336 g/mol (polystyrene equivalent).

(Bu−PPyV) is very soluble in typical organic solvents (i.e., THF, $CHCl_3$, and toluene) in both its neutral and protonated forms and is stable toward nucleophiles. The measured molecular weight of this polymer was 5200 g/mol. Figure 2 shows the molecular weight distribution of Bu−PPyV, where the horizontal axis gives the molecular weight of a polystyrene standard having identical elution time (equivalent hydrodynamic volume). On the low end of the molecular weight distribution, shoulders corresponding to discrete oligomer lengths are clearly visible. The spacing between these shoulders is nearly constant at 336 g/mol (polystyrene equivalent scale), and the position of the first clear shoulder (labeled 4 in Figure 2) is near 800 g/mol. The likely explanation for these observations is that the 2,5-dibromopyridine units rapidly dimerize in the reaction mixture, and it is the polymerization of these dimers that gives polymer. Rapid dimerization has been observed in this system previously.[35]

The electronic absorption spectra of spin-coated thin films of poly(*p*-pyridylvinylene) (PPyV) and two of its alkyl substituted derivatives (Me−PPyV and PMePyV) are shown in Figure 3. The wavelength of maximum absorption (λ_{max}) of the PPyV film is centered at 420 nm, while the λ_{max} of Me−PPyV is red-shifted to 450 nm. The electronic absorption spectrum of PMePyV is strongly blue-shifted (λ_{max} of 380 nm) relative to that of PPyV. The photoluminescence (PL) spectra of these polymer films are also shown in Figure 3. The PL spectra show similar shifts to those observed in the absorption spectra. With an excitation wavelength of 420 nm, the PPyV spectrum gives a peak in the emission spectrum at 590 nm, indicating orange-red emission. In comparison, the maxima in the PL spectra of Me−PPyV and PMePyV are at 630 and 540 nm, respectively. The electronic absorption spectra of polymer solutions and films are almost superimposable (e.g., compare the absorption spectra shown in Figures 3a and 6a], while the PL spectra of polymer solutions and films differ significantly (e.g., compare the PL spectra in Figures 3a and 6a]. In general, the thin film PL spectra have a broader line shape and are red-shifted by 100 nm relative to the solution spectra. The same sorts of shifts

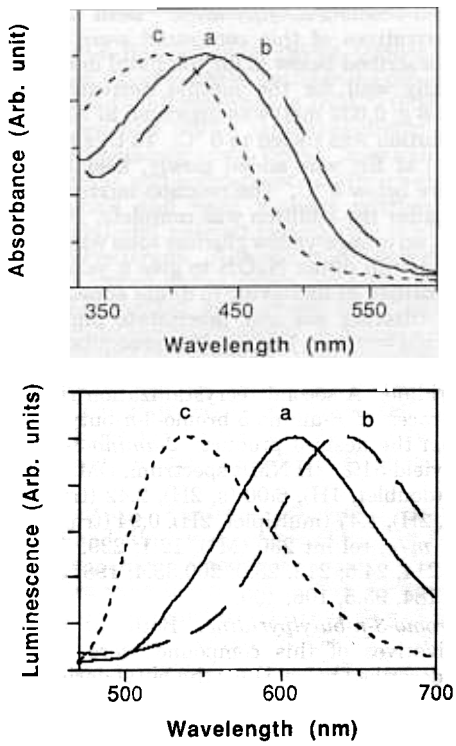

Figure 3. The plot at the top shows electronic absorption spectra of thin films of PPyV (curve a), Me-PPyV (curve b), and PMePyV(curve c) spin-coated onto glass substrates. The plot at the bottom shows photoluminescence spectra of PPyV (curve a), Me-PPyV (curve b), and PMePyV (curve c) of the same samples.

between solution and solid state spectra are observed in Bu−PPyV (vide infra). These results suggest excimer formation in the polymer films. A polymer can form two kinds of excimers: either between two neighboring polymer chains (interchain) or between different segments of the same polymer chain (intrachain). Since PPyV is expected to be a rigid polymer,[40,41] interchain excimers are more likely and have been observed in other systems.[41] In dilute solutions, the polymer chains are well separated and the probability of excimer formation is small, while in the polymer film excimers are much more probable. For PMePyV the solution and thin film spectra (both absorption and PL) are almost identical. In PMePyV, the pyridinium structure is formed quantitatively, and repulsion between the charged pyridinium units prevents the formation of excimers.

The high solubility of Bu−PPyV allows us to examine the emission spectra and lifetimes at a range of different solution concentrations, to look for the onset of excimer formation. The emission spectra of Bu−PPyV in THF solution (excitation wavelength = 420 nm) at different concentrations are shown in Figure 4. The spectra and the peak position change dramatically with concentration. In a dilute solution (e.g., 10^{-6} M based on monomer repeat unit), the spectrum shows maxima at 485 and 525 nm and a shoulder at 575 nm. The energy spacing of these bands (ca. 1600 cm^{-1}) is similar to that observed in other conjugated polymers and is most likely due to vibronic fine structure of the electronic transition. As the solution concentration increases, the PL maxi-

(40) Carter, P. W.; DiMagno, S. G.; Porter, J. D.; Streitwieser, A. *J. Phys. Chem.* **1993**, *97*, 1085.
(41) Jenekhe, S. A.; Osaheni, J. A. *Science* **1994**, *265*, 765.

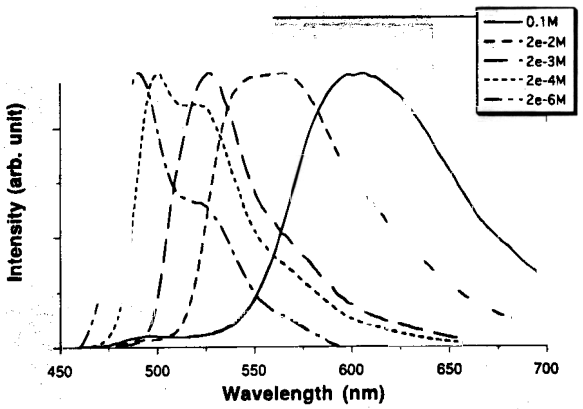

Figure 4. Photoluminescence spectra of Bu-PPyV in THF at concentrations of (a) 2×10^{-6}, (b) 2×10^{-4}, (c) 2×10^{-3}, (d) 2×10^{-2}, and (e) 0.1 M (concentration based on monomer unit).

mum shifts to longer wavelengths and broadens. The PL spectrum of a thin film of Bu–PPyV is identical to that of the 0.1 M solution. The progressive evolution of broad and structurless emission at high concentration from the highly structured emission for dilute solutions has been attributed to the formation of excimers.[41–43] It should be pointed out that as the polymer concentration increases, the high optical density of the solution will also contribute to the observed spectral shift, due to reabsorption of the emitted light, i.e., the inner filter effect.[37,43,44] In the standard configuration for measuring solution fluorescence spectra (excitation and detection at right angles to each other) the light emitted from isolated segments of the polymer is reabsorbed and either reemitted from excimeric states or lost to nonradiative relaxation. The light emitted from excimeric states is not reabsorbed and will thus escape the sample. To minimize the inner filter effect, the emission spectra were also measured with the front face excitation and emission (excitation is applied and emission collected on the same side of the sample). The spectra collected in this configuration are identical to the PL spectrum of the dilute solution (Figure 4a) with only minor red shifts at the higher polymer concentrations. Luminescence from an excimeric state is not observed in the front face configuration. The quantum efficiency for excimer fluorescence is much lower than that observed for isolated molecules or polymer segments.[42,43] In the front-face configuration the light emitted from monomer states is not reabsorbed before exiting the sample, and this emission dominates the observed spectra due to its greater quantum efficiency. Time resolved fluorescence decay was also measured in Bu–PPyV THF solutions, with right angle detection. At 10^{-5} and 10^{-6} M the lifetime is 630 ps, which increases to 1.1 ns at 10^{-3} M. At 0.1 M the relaxation is nonexponential and strongly quenched, supporting the existence of excimers at higher concentrations.

Similar experimental results were also observed in polymer blend films. Figure 5 shows the PL spectra of Bu–PPyV in poly(methyl methacrylate) (PMMA) at various concentrations. These polymer blends appear

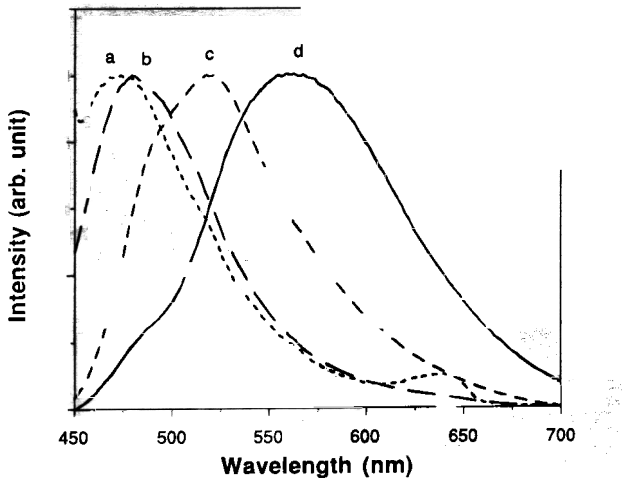

Figure 5. Photoluminescence spectra of Bu-PPyV in PMMA at concentrations of (a) 0.005 mol %, (b) 0.05 mol %, (c) 0.5 mol %, and (d) 2 mol % of Bu-PPyV.

optically to be homogeneous. This is somewhat surprising, since mixtures of two dissimilar polymers typically phase separate into mixtures with fairly large domains (>1 μm), which would lead to cloudy films.[45] We infer that any phase separation in these blends must occur at very small length scales (<0.1 μm). As shown in Figure 5, with about 2 mol % of Bu–PPyV present, the PL spectrum consists of a broad structurless line with a maximum at 580 nm. As the amount of Bu–PPyV decreases, the peak in the PL spectrum becomes narrower and shifts to a shorter wavelength (475 nm), corresponding to the trends in Bu–PPyV solutions at various concentrations. The electronic absorption spectra of the polymer films are identical regardless of the Bu–PPyV concentration within the films. These observations illustrate the existence of excimers in polymer solid solutions at high concentrations.

Treating PPyV, Me–PPyV, or Bu–PPyVwith strong acid gives the pyridinium salt of the polymer. Poly(pyridinium vinylene) (PHPyV) was prepared by adding methanesulfonic acid (MSA) or dodecylbenzenesulfonic acid (DBSA) to a *m*-cresol solution of PPyV. The degree of protonation can be controlled by the amount of acid added. As demonstrated in Figure 6 (top), with increasing acid concentration in the PPyV solution, the λ_{max} in the absorption spectrum shifts gradually toward longer wavelength. λ_{max} typically shifts from 410 to 430 nm as the acid concentration increases from 0 to 1 equiv of acid per repeating unit in the PPyV solution. The appearance of an isosbestic point in the electronic absorption spectra indicates the coexistence of PPyV and PHPyV polymer segments. The molar absorptivity of PHPyV is greater than that of PPyV, as demonstrated by the higher absorbance at λ_{max} for the protonated species. The PL spectra of the same polymers in *m*-cresol solutions are shown in Figure 6 (bottom). Relative to PPyV, a red-shift is observed in the spectra of poly(pyridinium vinylene) (PHPyV). The PL spectrum of the PPyV solution has a peak at 485 nm, while that of the partly protonated polymer solution (PHPyV/PPyV) has a peak at 550 nm, regardless of the acid concentration in the polymer solution. The quantum efficiency of PHPyV is lower than that of PPyV, and the

(42) Turro, N. J. *Modern Molecular Photochemistry*; Benjamin/Cummings: Menlo Park, CA, 1978.
(43) Guillet, J. *Polymer Photophysics and Photochemistry*; Cambridge University Press: Cambridge, 1985.
(44) Samuel, I. D. W.; Crystall, B.; Rumbles, G.; Burn, P. L.; Holmes, A. B.; Friend, R. H. *Chem. Phys. Lett.* **1993**, *213*, 472.
(45) Newman, D. R. P. S., Ed.; *Polymer Blends;* Academic Press, New York, 1978.

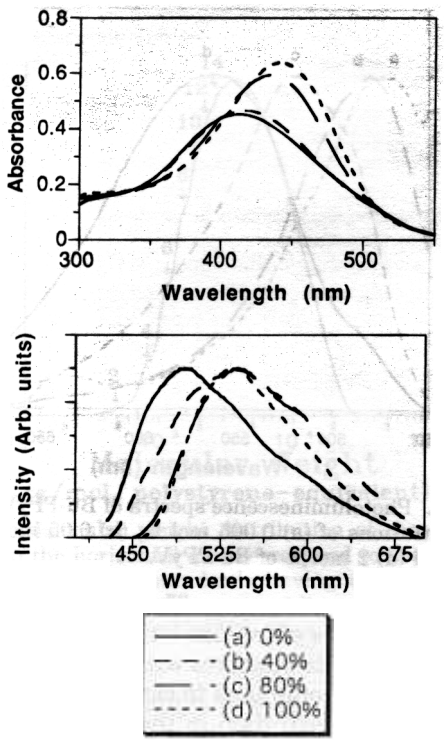

Figure 6. Electronic absorption spectra (top) and photoluminescence spectra (bottom) of PHPyV *m*-cresol solutions with protonation degree of (a) 0%, (b) 40%, (c) 80%, and (d) 100%.

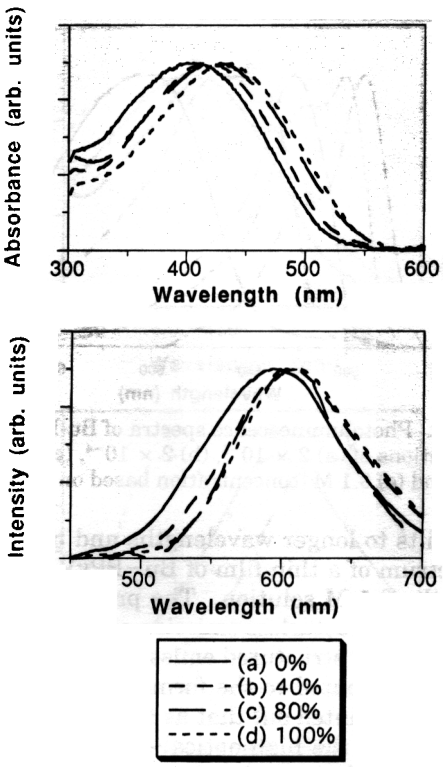

Figure 7. Electronic absorption spectra (top) and photoluminescence spectra (bottom) of PhPyV thin films with protonation degree of (a) 0%, (b) 40%, (c) 80%, and (d) 100%.

presence of excess acid significantly quenches the fluorescence. The quantum yields have been measured for Bu-PPyV; the PL quantum yield of Bu−PPyV in dilute THF is 0.9, and the quantum yield of Bu-PHPyV is about 0.7.[36] Red shifts relative to PPyV were also observed in films of PHPyV spin-coated from *m*-cresol, as illustrated in Figure 7.

The spectral shifts in the electronic absorption spectra of PHPyV, relative to PPyV, suggests a lower $\pi-\pi^*$ transition energy at the protonated site. The independence of the peak position in the PL spectrum of the degree of protonation indicates that the excitation energy decays through the same lower energy path, regardless of the structural composition of the polymer chain. This suggests that in the partly protonated PPyV chain, the excitation energy migrates through the polymer chain to a low energy site (i.e., the protonated site in polymer) and then radiatively decays to its ground state, as observed in other fluorescent polymers.[46] The PL spectrum thus becomes dominated by emission from the protonated portion of the chain. Using the same arguments given for PMePyV, samples of PHPyV would not be expected to form excimers due to electrostatic repulsions, but they do show strongly shifted emission in the solid state. Our best explanation of this is that even though an equivalent of acid has been added to solution, the polymer is not fully protonated.

Self-Assembled Polymer Thin Films. Many polyelectrolytes have been used to prepare multilayer polymer thin films via electrostatic deposition techniques.[21−26,47,48] The multilayer polymer thin films provide significant advantages over conventional polymer thin films, such as excellent uniformity in very thin films (20−500 Å) and a variety of film compositions. We have taken advantage of charged poly(*p*-pyridinium vinylene) to make polymer thin films with good optical properties.[49]

One of the driving forces for deposition of a polyelectrolyte from organic solvent is the electrostatic interaction between charged units in the polymer and an oppositely charged surface. Thin films of PHPyV and Bu−PHPyV were made by alternating dipping a cationically derivatized glass slide into a solution of an anionic polymer (i.e. sulfonated polyaniline (SPANI) or sulfonated polystyrene (PSS)) and cationic poly(pyridiunim vinylene) solutions. Solutions of PHPyV in *m*-cresol do not lead to any film growth, because *m*-cresol is a good solvent for the polymer. Adding a poorer solvent for PHPyV (i.e., acetonitrile) to *m*-cresol gives solutions that lead to efficient film growth. The uniformity of these multilayer polymer films was characterized by ellipsometry and atomic force microscopy (AFM). A PHPyV solution composed of 20% *m*-cresol and 80% acetonitrile gives a relatively rough film [root mean squared (RMS) roughness = 7 nm]. Films grown from a solution containing 40% *m*-cresol had much smoother surfaces, RMS roughness = 3 nm. In solutions rich in acetonitrile, the polymer chains appear to aggregate, leading to relatively rough films. Considering the relatively low molecular weight of the pyridyl vinylene polymers (ca. 5000 g/mol), the particle sizes that are evident in the AFM measurements correspond to many polymer strands lumped together. In contrast,

(46) Rauscher, U.; Bässler, H.; Bradley, D. D. C.; Hennecke, M. *Phys. Rev. B* **1990**, *42*, 9830.
(47) Keller, S. W.; Kim, H. N.; Mallouk, T. E. *J. Am. Chem. Soc.* **1994**, *116*, 8817.
(48) Kleinfield, E. R.; Ferguson, G. S. *Science* **1994**, *265*, 379.
(49) Tian, J.; Thompson, M. E.; Wu, C.-C.; Sturm, J. C.; Register, R. A.; Marsella, M. J.; Swager, T. M. *Polym. Prepr.* **1994**, *35*, 761.

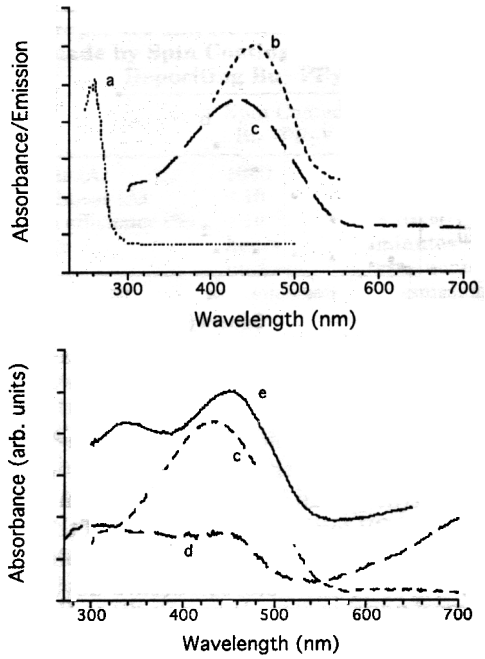

Figure 8. Electronic absorption spectra of (a) PSS, (b) PHPyV/PSS, (c) PHPyV$^+$MeSO3$^-$ thin film, (d) SPANI, (e) PHPyV/SPANI, and luminescence spectra of a PHPyV/PSS film (f).

the polymer chain is more strongly solvated and thus isolated in the solution containing a high percentage of *m*-cresol, leading to deposition of relatively smoother films. Films of Bu−PHPyV can be grown from a mixture of THF and acetonitrile and have an RMS roughness of 5 nm.

While the electrostatically deposited pyridylvinylene films are relatively flat, they are still much rougher than either spun coated films of Bu−PPyV or multilayer polymer films grown by electrostatic deposition from aqueous solutions. We have examined a PPV film grown with an aqueous solution of the cationic PPV precursor, as described by Fou et. al.[27] AFM was used to investigate films at both the precursor stage and after annealing to give the conjugated polymer. The RMS roughnesses estimated by AFM on 1 μm^2 sizes are very low (ca. 1 nm) for both types of film. The principal difference between the PPV and polypyridinium systems is the solvent (water versus an organic solvent). Water is preferable for obtaining flat films. The poor film forming properties of the organic solvent can be remedied somewhat by adding inorganic salts to bring up the ionic strength of the solution. It is found that in order to obtain a good quality film the ionic strength of the PHPyV solutions should be greater than 0.1 M. We are currently exploring derivatized polymers which will have sufficient water solubility and stability to allow us to make multilayer pyridylvinylene films from aqueous solutions.

The electronic absorption spectra of poly(*p*-pyridinium vinylene) multilayer thin films are shown in Figure 8. The absorption spectrum of PSS has an intense band in the ultraviolet (Figure 8a). The visible spectrum of a multilayer PHPyV/PSS film has a λ_{max} at 450 nm, and is very similar to a sample of the methylsulfonate salt of PHPyV (Figure 8c). SPANI shows bands at 320 and 460 nm as well as one centered in the near IR (Figure 8d). A PHPyV/SPANI multilayer film gives a spectrum which is a superposition of the spectra for the two

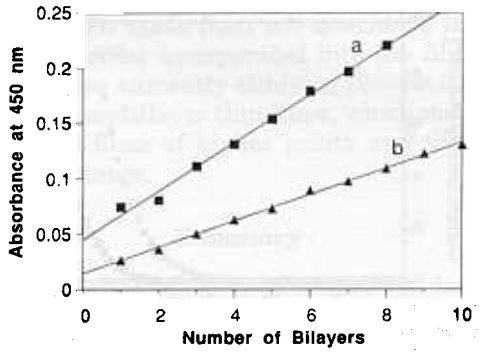

Figure 9. Plot of absorption at 450 nm versus number of Bu-PHPyV/PSS bilayers on (a) polyaniline and (b) PEI initiated ITO-coated glass slides.

polymers (Figure 8e). Both PSS and SPANI multilayer PHPyV films give a linear increase in absorbance as a function of the number of layers deposited (Figure 9). The data for figure 9 were collected in a day. Storing the films overnight leads to a decrease in absorbance at 450 nm.[36] When the film growth is resumed, the observed rate of growth is identical to that of the previous day.

Many factors influence the formation of self-assembled polymer thin films, such as the counter polyions and the nature of substrate. We have grown polymer layer-by-layer thin films on glass slides, silicon wafers, and indium/tin oxide (ITO) coated glass slides. Silane treated glass slides and Si wafers (cationic surfaces) promote very good adhesion of sulfonated polyaniline and sulfonated polystyrene. In the case of ITO coated glass, the silane treatment does not give reproducible results. This may be due to the limited number of hydroxyl groups on the ITO-covered glass surface, since the silane couples only to the hydroxyl groups. To overcome this problem, we have initialized the ITO-coated glass by in-situ deposition of conducting polypyrrole or polyaniline thin films,[25] which give uniform self-assembled polymer thin films (PHPyV/SPANI, PHPyV/PSSNa). ITO-coated glass initiated with poly(ethylene imine) (PEI) has been used to prepare polymer thin films.[27] Figure 9 is the plot of absorbance at 450 nm versus number of bilayers in the layer-by-layer thin films of Bu−PHPyV and PSS. While both polyaniline- and PEI-coated substrates give linear growth, the PEI-initiated film grows significantly slower. The slower rate of growth of PEI initiated films may be due to poor binding of PEI to the ITO surface leading to a patchy film.

We have been unsuccessful in growing Bu−PHPyV multilayer films with poly(methacrylic acid) and poly(acrylic acid) by electrostatic deposition. This could be due to a poor match of pK_a values, which leads to proton transfer from PHPyV to the acrylate polymers, giving neutral polymers which dissolve in the organic solutions.

Photoluminescence spectra of the pyridylvinylene multilayers were measured, and the spectrum of PHPyV/PSS is shown in Figure 8. The photoluminescent yields for Bu−PHPyV/SPANI films were much lower than for analogous Bu−PHPyV/PSS films. The band-gap of SPANI is lower than that of Bu−PHPyV; as a consequence, an exciton generated in Bu-PHPyV may migrate to the SPANI chain. Because of the large number of trap sites on the SPANI chain, the exciton

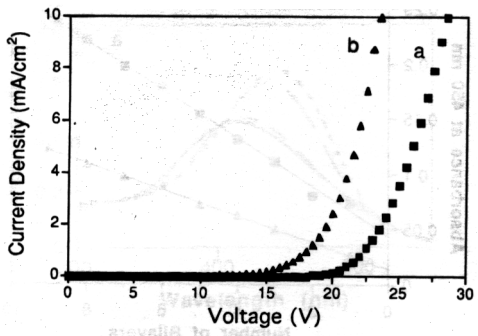

Figure 10. Current–voltage characteristics of (a) ITO/Bu-PPyV/Al and (b) ITO/PPV/Bu-PPyV/Al device.

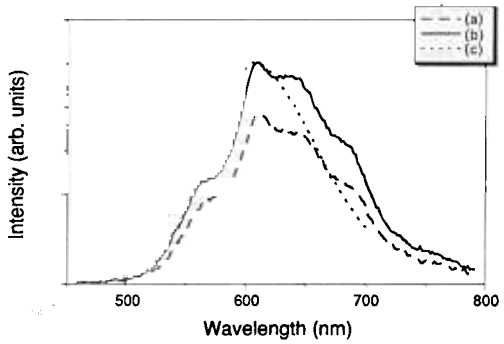

Figure 11. Electrochemiluminescence spectra of (a) ITO/Bu-PPyV/Al, and (b) ITO/PPV/Bu-PPyV/Al device, and (c) photoluminescence spectrum of Bu-PPyV film.

will decay nonradiatively, reducing the fluorescence quantum yield.[50,51] This process is absent in the Bu–PHPyV/PSS thin film, because of the much wider band gap in the PSS relative to that in Bu–PHPyV. The excitons thus remain localized on Bu–PHPyV. LEDs have been fabricated with Bu–PHPyV/PSS thin films previously and will be discussed in the next section.[49]

Light-Emitting Diodes. LEDs containing Bu–PPyV as the emissive layer have been fabricated by spin-coating the polymer solution in chloroform or THF onto ITO-coated glass substrates. Arrays of 1 mm² Al contacts were then evaporated on top of the polymer films. All devices were then operated in air at room temperature. Figure 10a shows the forward (ITO as positive) current–voltage (I–V) curve of an ITO/Bu–PPyV (1100 Å)/Al device. The light emission of the device starts to be visible between 28–30 V, showing uniform orange-red emission. The EL spectrum is shown in Figure 11a, essentially consistent with its PL spectrum in Figure 11c. The EL intensity vs. drive current is shown in Figure 12a. The EL intensity is roughly proportional to the drive current only up to 100 μA, with an external quantum efficiency of about 0.02%. The devices last for roughly 30 min under this current level. When the drive current is raised above 100 μA (10 mA/cm²), the EL intensity is no longer proportional to the drive current, and the device fails very rapidly, with the appearance of visual damage to the contacts, eventually leading to open circuits.

To improve the carrier injection into Bu–PPyV, a PPV hole transport layer, was introduced to form a heterostructure with the configuration ITO/PPV/Bu–PPyV/Al. The PPV layer was formed by spin-coating and thermally converting the PPV precursor on the ITO coated substrate. The Bu–PPyV was then spin-coated on top of the PPV layer. The thickness of the PPV layer is about 300 Å and the total thickness is about 1500 Å. The I–V curve of the heterostructure device is shown in Figure 10b, in comparison with the single layer device. Though the total thickness is larger in the heterostructure device, it shows a 5–6 V reduction in the operation voltage. The heterostructure device emits orange-red light, and its EL spectrum in Figure 11b is identical to that of the single layer device, without any evidence of emission from the PPV layer. This contrasts greatly with our previous work on PPV/Alq heterostructures, in which light from both PPV and Alq was seen at all bias levels.[52] This effect is caused by the relative bandgaps for excitons in the two materials. The exciton energies in PPV and Alq are similar, both having a peak emission around 550 nm, while the exciton for PPV is higher in energy that of Bu–PPyV (green vs orange-red luminescence, respectively). In the PPV/Alq case excitons may diffuse between the two materials with little energy change, but they are confined to Bu–PPyV with respect to PPV because of their lower energy. Similar effects are seen in other polymeric[53–55] and molecular[18,56–60] heterostructured devices as well.

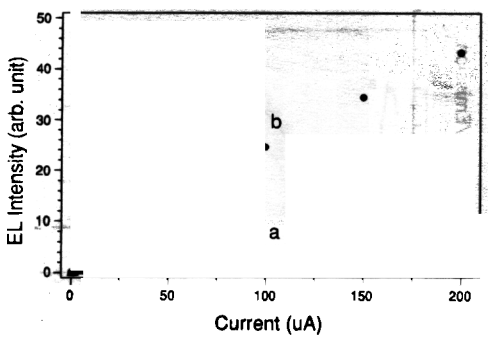

Figure 12. Light emission versus applied bias for (a) ITO/Bu-PPyV/Al and (b) ITO/PPV/Bu-PPyV/Al devices.

As shown in Figure 12b, the introduction of PPV increases the light emission by a factor of 3, leading to an initial external quantum efficiency of 0.05% for the heterostructure device. The heterostructure also prolonged the lifetime of the devices. Under the drive current of 100 μA, the EL intensity dropped to about half of its initial value in a period of one hour, in contrast to 10 min for the single-layer device. The decrease of the operation voltage and the increase of

(50) Kim, Y. H.; Phillips, S. D.; Nowak, M. J.; Spiegel, D.; Foster, C. M.; Yu, G.; Chiang, J. C.; Heeger, A. J. *Synth. Met.* **1989**, *29*, E291.
(51) Kim, Y. H.; Foster, C. M.; Chiang, J. C.; Heeger, A. J. *Synth. Met.* **1989**, *29*, E285.
(52) Wu, C. C.; Chun, J. K. M.; Burrows, P. E.; Sturm, J. C.; Thompson, M. E.; Forrest, S. R.; Register, R. A. *Appl. Phys. Lett.* **1995**, *6*, 653–655.
(53) Colvin, V. L.; Schlamp, M. C.; Alivisatos, A. P. *Nature* **1994**, *370*, 354–357.
(54) Holmes, A. B.; Bradley, D. D. C.; Brown, A. R.; Burn, P. L.; Burroughes, J. H.; Friend, R. H.; Greenham, N. C.; Gymer, R. W.; Halliday, D. A.; Jackson, R. W.; Jackson, R. W.; Kraft, A.; Martens, J. H. F.; Pichler, K.; Samuel, I. D. W. *Synth. Met.* **1993**, *55–57*, 4031–4040.
(55) Uchida, M.; Ohmori, Y.; Noguchi, T.; Ohnishi, T.; Yoshino, K. *Jpn. J. Appl. Phys.* **1993**, *32*, L921-L924.
(56) Tang, C. W.; VanSlyke, S. A. *Appl. Phys. Lett.* **1987**, *51*, 913.
(57) Tang, C. W.; VanSlyke, S. A.; Chen, C. H. *J. Appl. Phys.* **1989**, *65*, 3610.
(58) Ohmiri, Y.; Fujii, A.; Uchida, M.; Morishima, C.; Yoshino, K. *Appl. Phys. Lett.* **1993**, *63*, 1871.
(59) Hosokawa, C.; Higashi, H.; Kusumoto, T. *Appl. Phys. Lett.* **1993**, *62*, 3238.
(60) Burrows, P. E.; Forrest, S. R. *Appl. Phys. Lett.* **1994**, *64*, 2285.

Table 1. Properties and Device Parameters for Similar Devices Made by Spin Coating and Electrostatically Depositing Bu–PPyV

	Spin Coated Bu–PPyV	Multilayer Bu–PHPyV/PSS
film thickness (Å)	1000	400
surface roughness (Å)	<10	≈50
EL quantum efficiency (%)	$>10^{-2}$	$<10^{-3}$
lifetime in air	hours	minutes
observation	uniform emission	very nonuniform emission, twinkling spots

efficiency suggest that the hole injection is improved in the heterostructure device. This suggests that PPV is a better hole injector and transport layer than Bu–PPyV, or there is a better match between the work function in the ITO and the highest energy filled state (HOMO) in PPV than that in Bu–PPyV, leading to a smaller energy barrier for hole injection. The presence of PPV with a larger energy gap may also confine excitons in Bu–PPyV and therefore away from the ITO interface, which is a nonradiative quenching site, leading to higher efficiency.

Our initial data on LEDs fabricated from the self-assembled Bu–PHPyV/PSS films were reported elsewhere.[36] The multilayers were deposited on ITO, and Al was used as the top contact. Table 1 contrasts the performances of LEDs prepared from electrostatic self-assembled films and those from spin-coated Bu–PPyV films. There was no thermal treatment after the deposition of polymers in either case and all measurements were performed in air at room temperature. The external EL quantum efficiencies of self-assembled devices and spin-coated devices are <0.001% and >0.02%, respectively. Further, the lifetime is on the order of minutes for the self-assembled devices vs hours for the spin-coated devices. Emission over the device area of the self-assembled device is very nonuniform, with twinkling spots, while that of the spin-coated devices was uniform. The poor performance of the self-assembled devices may be due to their relatively large surface roughness, ~5 nm for the self-assembled films vs ≤1 nm for the spin-coated films. The roughness leads to very nonuniform cathodes and a nonuniform electric field. Spots with high fields conduct a high current density and could form local "hot spots", which would lead to the rapid degradation of the self-assembled devices. Another possible cause for the poor performance of OLEDs made from self-assembled thin films could be impurities incorporated into the film during growth. We are currently studying different methods to deposit the multilayer thin films, which may lead to more uniform films of higher purity and thus better device performance.

Summary

Poly(*p*-pyridylvinylene) (PPyV) and its derivatives have been synthesized and their optical properties have been studied in solutions and thin films. These conjugated polymers luminesce strongly in both their neutral and protonated forms from excimeric states, which contributes to the observed red shift in the emission spectra and the low PL quantum yields. Self-assembled polymer thin films of poly(pyridinium vinylene) with sulfonated polystyrene or sulfonated polyaniline have been prepared by the electrostatic deposition method. Various deposition conditions were investigated and the films examined by atomic force microscopy (AFM), showing them to be significantly rougher than spin-coated films of PPyV.

Light-emitting devices (LEDs) with several different architectures were made from the pyridylvinylene polymers and evaluated. The polymer thin films were spin-coated from solution and the devices emit generally orange-red colors consistent with their PL spectra. The device made from poly(3-*n*-butyl-*p*-pyridylvinylene) with the configuration ITO/Bu–PPyV/Al has an external quantum efficiency of 0.02%. The introduction of a hole transport layer (poly(*p*-phenylenevinylene), PPV) between the Bu–PPyV and ITO layer improves the quantum efficiency of the device (up to 0.05%), reduces the operating voltage and prolongs the lifetime of the device.

Acknowledgment. This work was supported by the New Jersey Commission of Science and Technology through the Advanced Technology Center for Photonic and Optoelectronic Materials (ATC/POEM), the Princeton Materials Institute (PMI), and the American Biomimetics Corp. The authors would like to thank Dr. Alex Siemiarczuk (Photon Technology International, London, Ontario, Canada) for measuring lifetimes and front face excitation fluorescence spectra.

CM950286K